Investigation of the Magnetic Field Configuration for Magnetic Surface Measurements in the CFQS Quasi-Axisymmetric Stellarator*)

Mamoru SHOJI[1,2], Akihiro SHIMIZU[1,2], Shigeyoshi KINOSHITA[1], Shoichi OKAMURA[1], Yuhong XU[3] and Haifeng LIU[3]

[1] *National Institute for Fusion Science, National Institutes of Natural Sciences, 322-6 Oroshi-cho, Toki 509-5292, Japan*

[2] *The Graduate University for Advanced Studies (SOKENDAI), Shonan Village, Hayama 240-0913, Japan*

[3] *Institute for Fusion Science, School of Physical Science and Technology, Southwest Jiaotong University, Chengdu 610031, China*

(Received 8 January 2023 / Accepted 7 March 2023)

It has been found that magnetic surfaces in the CFQS quasi-axisymmetric stellarator in a standard magnetic configuration are robust against error fields caused by misalignments of the modular coils. While this property is advantageous for preserving the magnetic field line structures for the plasma confinement as designed, it prevents the detection of the misalignments of the coils by magnetic surface measurements. Thus, a magnetic configuration specialized in measuring magnetic surfaces to detect the error fields is proposed. Calculations by tracing magnetic field lines reveal that the magnetic surfaces in the specialized magnetic configuration are sensitive to the error fields compared to those in the standard magnetic configuration. Additionally, the calculations demonstrate that a weighted electric current on some modular coils can make the magnetic surfaces more sensitive to the error fields, which enables the magnetic surface measurements to detect smaller misalignments of the modular coils in the CFQS.

Keywords: magnetic surface, magnetic field line mapping, magnetic island, error field, CFQS

DOI: 10.1585/pfr.18.2405026

1. Introduction

A quasi-axisymmetric stellarator, CFQS, has now been constructed as a joint project between National Institute for Fusion Science and Southwest Jiaotong University [1]. The CFQS is a low-aspect-ratio stellarator based on CHS-qa [2]. The main parameters of the CFQS are as follows: the major radius (R) is 1 m, the toroidal magnetic field in a high magnetic field operation (B_t) is 1 Tesla, the toroidal periodic number (N_p) is 2, and the aspect ratio (A_p) is 4. The magnetic coil system consists of sixteen modular coils (MCs), four poloidal field coils (PFCs), and twelve toroidal field coils (TFCs) [3]. The MCs, which have complicated shapes and a large total electric current, are one of the major components of the CFQS. There are four differently shaped MCs connected to four independent electric power supplies. They are for controlling the mirror ripple to intentionally break the quasi-axisymmetric symmetry of the magnetic configuration for investigating the plasma confinement physics and so on. The PFCs are installed to change the position of the magnetic axis in the plasma confinement region in the major radius by applying the vertical component of the magnetic field. Two pairs of PFCs (named IV and OV coils) are installed in the inboard and outboard sides of the torus, respectively.

Experiments for measuring magnetic surfaces (so-called magnetic field line mapping) are planned just after the completion of the construction of the CFQS. The purpose of the experiments is to confirm the formation of magnetic field line structures for plasma confinement and the completeness of the magnetic coil installation. A fluorescent method [4–7] is planned to be adopted in the experiments for magnetic surface measurements. A mesh, which fully covers the poloidal cross-section of the plasma confinement region, is inserted into the vacuum vessel through a large rectangular outer port. A fluorescent material (ZnO: zinc oxide) is sprayed onto the surface of the wires for the mesh. A small-sized electron gun is vertically inserted into the plasma confinement region in the vacuum vessel from a lower port. An electron beam is extracted from the aperture of the electron gun along the magnetic field line. The extracted electron beam toroidally circulates, and it collides with fluorescent material on the wires, which produces visible fluorescent lights at the collision points on the mesh. The positions of the fluorescent light are recorded with a high-sensitivity camera which is mounted at an outer port

author's e-mail: shohji.mamoru@nifs.ac.jp

*) This article is based on the presentation at the 31st International Toki Conference on Plasma and Fusion Research (ITC31).

tangentially viewing the mesh. The recorded image of the fluorescent lights provides information on the poloidal cross-section of a magnetic surface. The magnetic surfaces at different minor radii are measured by changing the position of the electron gun. During the exposure time of the high-sensitivity camera, the fluorescent mesh is slightly moved in the major radius. The moving distance is equivalent to the gap between the wires on the mesh. It is expected that this technique enables to record the images of magnetic surfaces with high spatial resolution.

An investigation by tracing magnetic field lines in the plasma confinement region has revealed that the magnetic surfaces in a standard magnetic configuration are robust against the error magnetic fields caused by misalignments of the MCs [8], in which the structure of the magnetic surfaces is almost unchanged by the misalignments. While this property is advantageous for preserving the magnetic surfaces as designed, it prevents the detection of the error fields. To ascertain the misalignment of the coils, a magnetic configuration specialized in magnetic surface measurements has to be found, in which the structure of the magnetic surfaces has to be sensitive to the error fields. The PFCs can be used not only to change the position of the magnetic axis but also to control the radial profile of the rotational transform so as to cross rational surfaces, forming magnetic islands in the plasma confinement region. Since it is well known that the structure of the magnetic islands is sensitive to error fields, the misalignment of the coils can be detected by measuring the magnetic islands.

In the next section, the setup for the calculation of the magnetic surfaces by tracing magnetic field lines is presented. In section 3, a magnetic configuration specialized in magnetic surface measurements is proposed. In section 4, the calculations of the magnetic surfaces, including the error fields caused by displacements of one of the MCs in the major radius, are presented. It shows that the displacements of some modular coils are not detectable even in the specialized magnetic configuration. In section 5, a new magnetic configuration with a weighted electric current on some MCs is proposed for detecting the displacements of the coils, which successfully solves the issue of the magnetic surface measurements in the specialized magnetic configuration.

2. Setup for the Calculation of the Structure of the Magnetic Surfaces in the CFQS

The calculations of the structure of the magnetic surfaces were performed by plotting the positions of magnetic field lines passing through the poloidal plane on which the fluorescent mesh is installed. The magnetic field lines in the plasma confinement region were traced using a single filament model of the magnetic coils in the CFQS. In this model, the finite-sized magnetic coils were approximated as single loops. Figure 1 (a) illustrates a perspective view of the model, in which the sixteen MCs and the four PFCs are shown. For simple calculation, it was assumed that the shape and position of the PFCs were set as designed (no displacement of the PFCs was assumed). Figure 1 (b) depicts the top view of the model, showing the toroidal location of the four differently shaped MCs. In this paper, the displacement of one of the MCs in the major radius was assumed as one of the most probable misalignments of the coils. The purpose is to investigate the influence of the radial displacement of the coil on the magnetic surfaces in the plasma confinement region in the CFQS.

The initial positions for tracing the magnetic field lines were set along a line on which the electron beam is extracted by changing the position of the electron gun in the minor radius. The toroidal position of the electron gun was set around the opposite side of the mesh and the camera, as illustrated in Fig. 1 (b). The electron gun has to be installed as far as possible from the mesh to minimize the

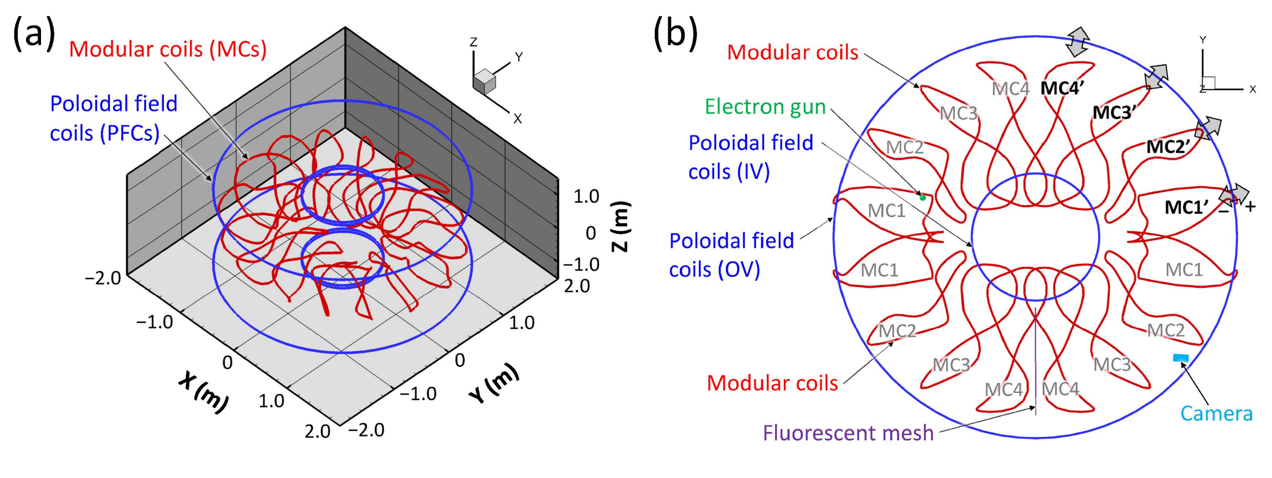

Fig. 1 (a) A perspective view of a single filament model of the magnetic coils in the CFQS. (b) A top view showing the positions of four differently shaped modular coils (MCs) which are named MC1, MC2, MC3, and MC4. Two pairs of poloidal field coils (PFCs) are indicated as IV and OV coils. The MCs which are displaced in the major radius are designated MC1′, MC2′, MC3′, and MC4′. The positions of the electron gun, the fluorescent mesh, and the high-sensitivity camera are also shown in this figure.

stray light emitted from the aperture of the electron gun. This is because the stray light reflected on the vacuum wall at the back of the mesh can disturb the magnetic surface measurements with the high-sensitivity camera. The shape of the magnetic surfaces at the toroidal position of the mesh is horizontally elongated in the standard magnetic configuration in which the electric currents are not applied to PFCs and TFCs.

In the calculation, the electric current of all MCs was set to 27.3 kA·T, which is a typical value for sustaining the magnetic field for two minutes in a steady state. The strength of the toroidal magnetic field at the magnetic axis (B_t) was 0.1 Tesla in this steady-state operation which is necessary for measuring magnetic surfaces. The effect of the earth magnetism at Chengdu in China (the construction site) was included in these calculations.

3. Magnetic Configuration Specialized in the Magnetic Surface Measurements

The calculated magnetic surfaces in the standard magnetic configuration are shown in Fig. 2 (a). The poloidal cross-section of the magnetic field lines at the fluorescent mesh is illustrated in this figure. In this magnetic configuration, the range of the rotational transform in the plasma confinement region (under the vacuum condition) is between less than 0.40 (at the magnetic axis) and ~0.35 (in the periphery), in which the radial profile of the rotational transform does not cross low-order rational surfaces [8]. In this calculation, the initial position for tracing magnetic field lines was changed by 5 mm in the minor radius. It has been recognized that the standard magnetic configuration is not appropriate for magnetic surface measurements because the structure of the magnetic surfaces is hardly changed by the misalignments of the MCs [9]. It has been found that a large vertical displacement of some groups of MCs by 20 mm causes a change in the radial profile of the rotational transform to form magnetic islands in the standard magnetic configuration [3].

Magnetic islands are intrinsically formed at the rational surfaces in non-axisymmetric magnetic plasma confinement devices such as heliotron and stellarators [10]. The islands are also produced by error fields due to the misalignment of the magnetic coils. The structure of the magnetic islands is sensitive to error fields. Here, a magnetic configuration specialized in magnetic surface measurements is proposed, in which magnetic islands are intentionally produced by applying the magnetic field of the PFCs to that in the standard magnetic configuration. In addition, the PFCs are cooled by water not by air, enhancing the operation rate of the experiments, thanks to the shorter cooling time of the coils. The electric currents of the IV and OV coils were set to −7.3 kA·T and +7.3 kA·T in the specialized configuration, respectively. Here the positive and negative values indicate the electric currents clockwise and counterclockwise in these two coils when viewed from the above, respectively. The range of the radial profile of the rotational transform in this magnetic configuration is between ~0.36 (at the magnetic axis) to ~0.32 (in the periphery), which crosses a major low-order rational surface of $q = 1/3$ in the plasma confinement region, where q is a safety factor of field lines on the magnetic surfaces. Figure 2 (b) presents the calculated magnetic surfaces in this configuration. Up-down symmetric magnetic islands ($m/n = 6/2$) about the equatorial plane ($Z = 0.0$ m) are formed in the plasma confinement region, where m and

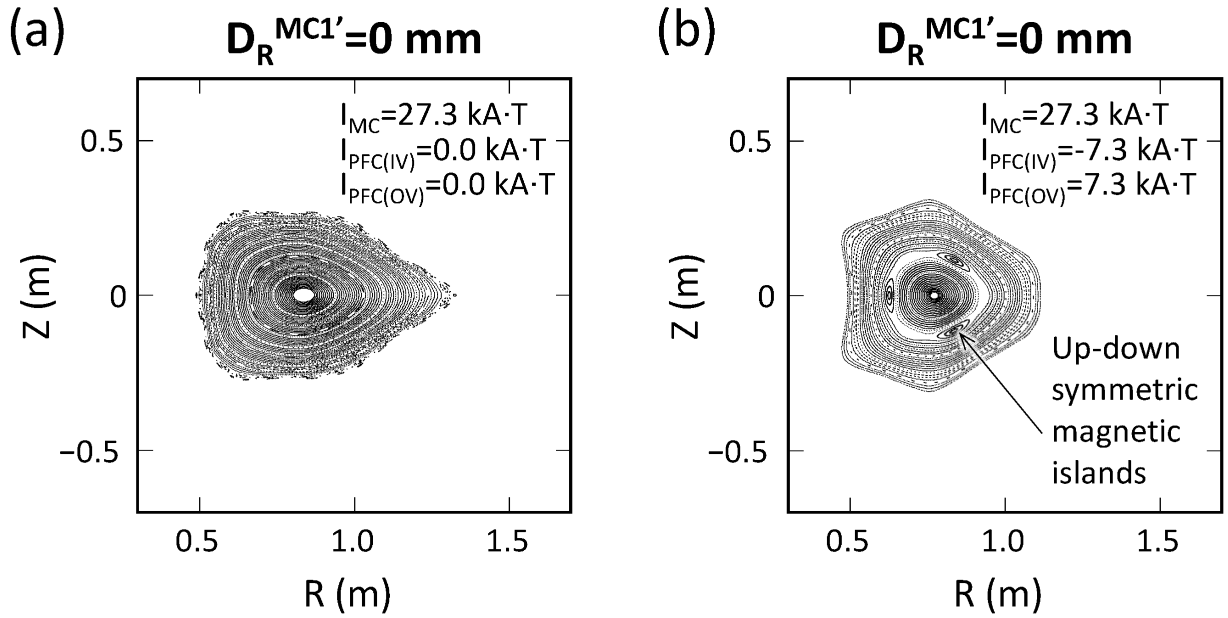

Fig. 2 The calculated magnetic surfaces on the poloidal plane at the fluorescent mesh in a low magnetic field (B_t = 0.1 Tesla) in the standard magnetic configuration (a) and the specialized magnetic configuration for magnetic surface measurements (b).

n represent poloidal and toroidal mode numbers, respectively. It should be noted that only three magnetic islands out of six ones are shown in Fig. 2 (b). The reason for this is that the tracing of the magnetic field lines on the fluorescent mesh is started from the initial positions on the movable range of the electron gun. Figure 3 gives the poloidal cross-section of the magnetic surfaces at the toroidal position where the movable electron gun is installed in the specialized magnetic configuration. A solid blue line indicates the movable range of the electron gun. The magnetic surfaces are measured while changing the position along this line which crosses only one magnetic island connecting with the three magnetic islands on the mesh.

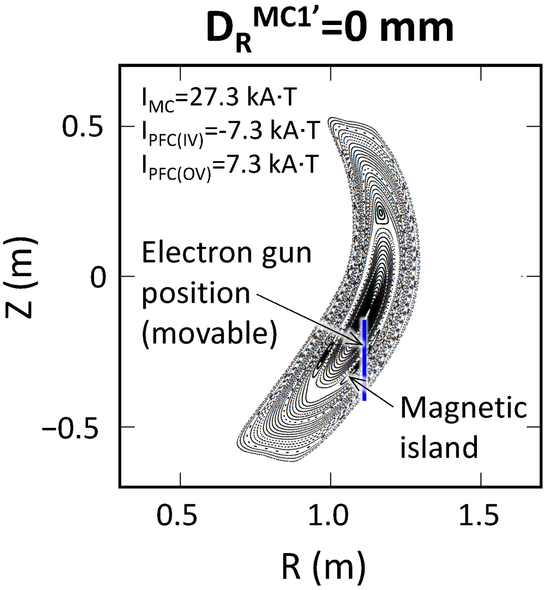

Fig. 3 The poloidal cross-section of the calculated magnetic surfaces in the specialized magnetic configuration for magnetic surface measurements in a low magnetic field (B_t = 0.1 Tesla) at the toroidal position where the electron gun is installed. A solid blue line indicates the positions of the range of the movable electron gun. Only three magnetic islands out of six ones are shown in this figure.

For verifying the sensitivity of the structure of the magnetic islands to the error fields in the specialized configuration, the magnetic surfaces were calculated when one modular coil MC1′ was displaced by 10 mm outward in the major radius. The toroidal position of the MC1′ is indicated in Fig. 1 (b). Figures 4 (a) and (b) depict the calculated magnetic surfaces in the standard and the specialized configurations, respectively. The magnetic surfaces in the standard magnetic configuration (Fig. 4 (a)) are hardly changed from those in the case without the displacement of the coil (Fig. 2 (a)). On the other hand, in the specialized magnetic configuration, up-down asymmetric magnetic islands are produced in the plasma confinement region. These calculations prove that the up-down asymmetry of the structure of the magnetic islands can be used as a good indicator to detect the error fields caused by the misalignment of the MCs.

4. The Influence of the Misalignment of Modular Coils on the Magnetic Surfaces

The influence of the misalignment of MCs was investigated by calculating the magnetic surfaces under conditions where the radial position of one MC was displaced

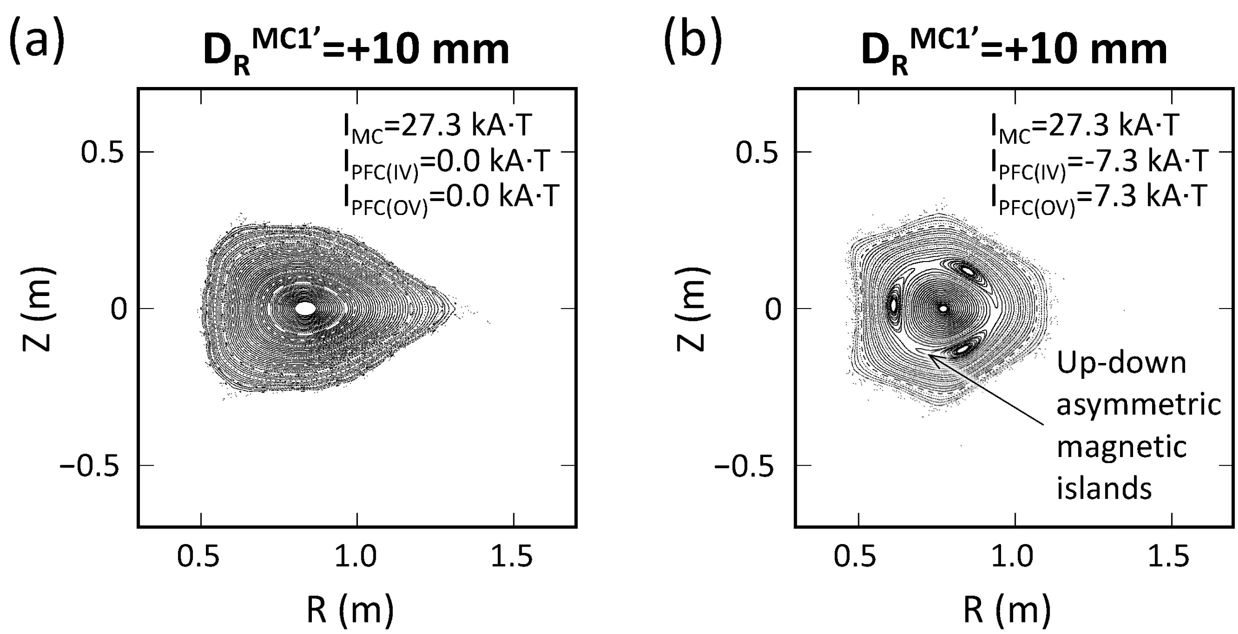

Fig. 4 The calculated magnetic surfaces on the poloidal plane at the fluorescent mesh in the case with a displacement of one modular coil MC1′ by +10 mm (outward in the major radius) in the standard magnetic configuration (a) and the specialized magnetic configuration for the magnetic surface measurements (b).

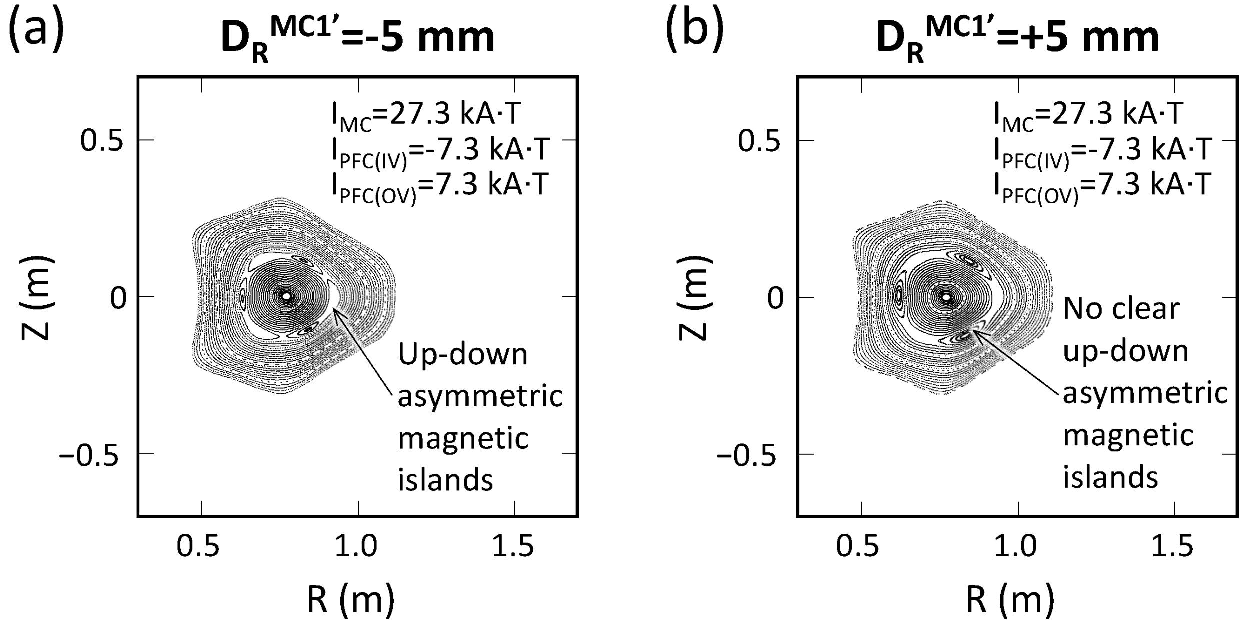

Fig. 5 The calculated magnetic surfaces in the specialized magnetic configuration with radial displacements of one modular coil MC1′ by −5 mm (inward in the major radius) (a) and +5 mm (outward) (b).

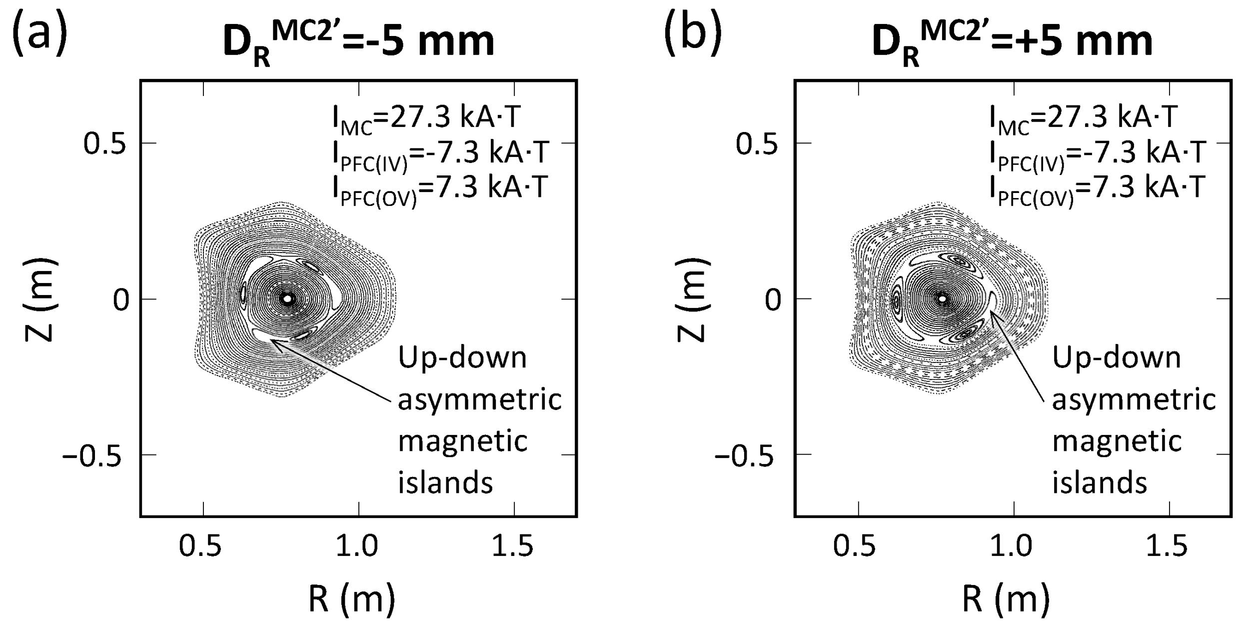

Fig. 6 The calculated magnetic surfaces in the specialized magnetic configuration with radial displacements of one modular coil MC2′ by −5 mm (a) and +5 mm (b).

in the major radius. The effect of the misalignment of the four differently shaped MCs (MC1, MC2, MC3, and MC4) was analyzed by changing the radial positions of MC1′, MC2′, MC3′, and MC4′, respectively, which toroidal positions are indicated in Fig. 1 (b). Here a small displacement of 5 mm in the major radius was considered as one of the possible misalignments of the coils. Figures 5 (a) and (b) display the calculated magnetic surfaces when the position of the MC1′ was moved by −5 mm (inward displacement in the major radius) and +5 mm (outward displacement), respectively. While the structure of the magnetic islands is up-down asymmetric about the equatorial plane ($Z = 0.0$ m) for the inward displacement (Fig. 5 (a)), the asymmetry is not clear for the outward displacement (Fig. 5 (b)). In other words, the magnetic islands for the outward displacement are almost identical to those for no displacement (Fig. 2 (b)). These calculations demonstrate that while a radial displacement of MC1′ by −5 mm is detectable by measuring the magnetic island structure, a radial displacement of MC1′ by +5 mm cannot be detected

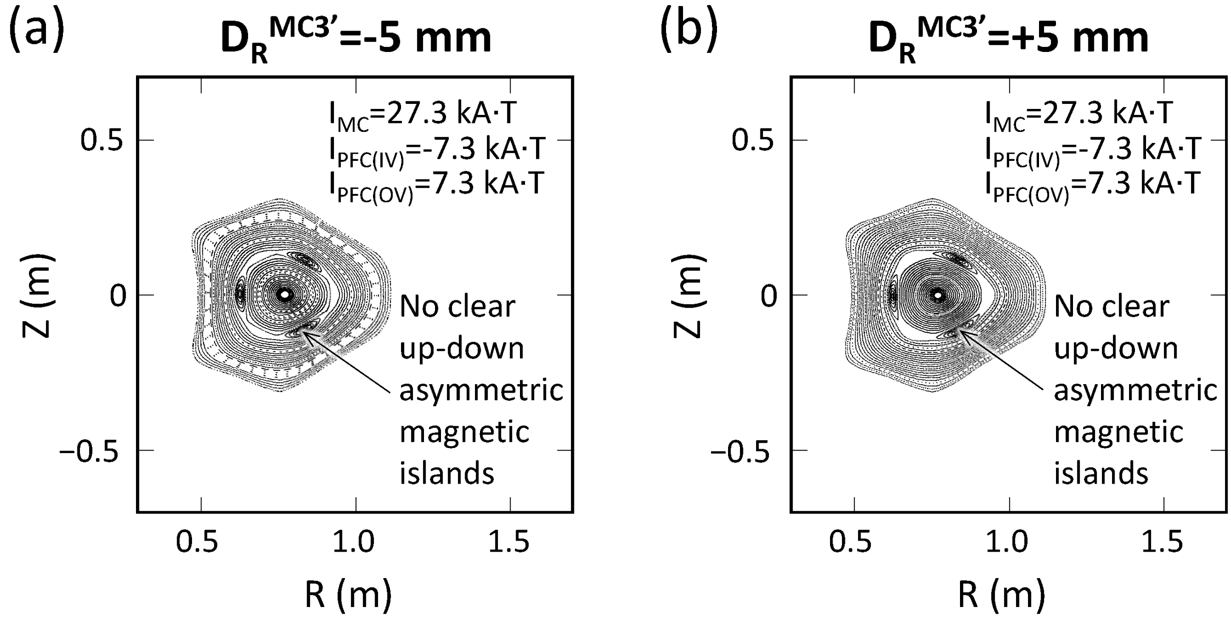

Fig. 7 The calculated magnetic surfaces in the specialized magnetic configuration with radial displacements of one modular coil MC3′ by −5 mm (a) and +5 mm (b).

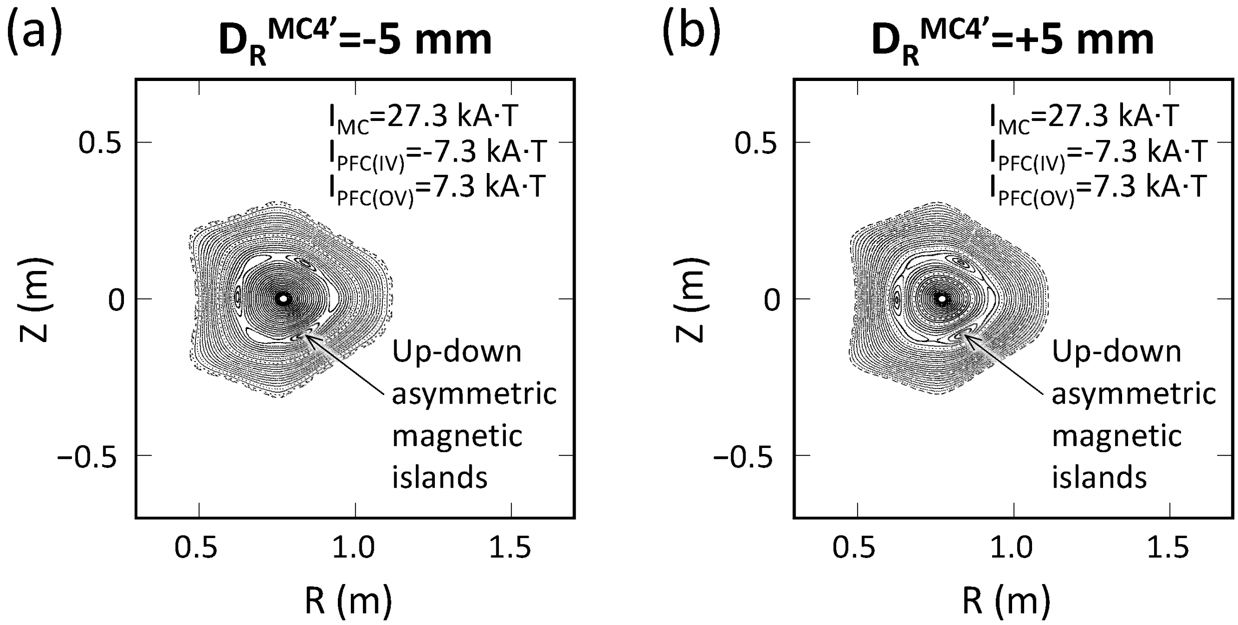

Fig. 8 The calculated magnetic surfaces in the specialized magnetic configuration with radial displacements of one modular coil MC4′ by −5 mm (a) and +5 mm (b).

even in the specialized magnetic configuration.

It should be noted that the positions of the O-points of the observed magnetic islands are not sensitive to the error field, which means the positions of the O-points are not useful for detecting error fields. The position of the X-points of the observed islands also cannot be adopted as an indicator to quantitatively evaluate the error field. This is because the poloidal positions of the X-points significantly change depending on whether the observed magnetic structure around the magnetic islands contains three or six islands. The poloidal positions are largely moved by the position of the electron gun as shown in Figs. 5 (a) and (b). Thus, in the following in this paper, the availability of the up-down asymmetry of the observed magnetic islands is discussed just for detecting the error fields due to the radial displacement of MCs.

Figures 6 (a) and (b) present the calculated magnetic surfaces for displacements of the MC2′ by −5 mm and

+5 mm, respectively. They show the up-down asymmetry of the magnetic islands in both cases, indicating that radial displacements of the MC2′ by ±5 mm are detectable in the specialized magnetic configuration. Figures 7 (a) and (b) display the calculations for displacements of the MC3′ by −5 mm and +5 mm, respectively. These figures show no clear up-down asymmetry of the magnetic islands in both cases, which means that the radial displacements of MC3′ by ±5 mm are difficult to detect by the magnetic surface measurements even in the specialized magnetic configuration. Figures 8 (a) and (b) depict the calculations for displacements of the MC4′ by −5 mm and +5 mm, respectively. They present up-down asymmetry of the magnetic islands in both cases, which proves that the displacements of the MC4′ of ±5 mm can be found in the specialized magnetic configuration.

5. Magnetic Configuration for the Magnetic Surface Measurements with a Weighted Electric Current on Modular Coils

The calculations in the last section demonstrate that a radial displacement of the modular coil MC1′ by +5 mm is hard to detect even in the specialized magnetic configuration. It was found that the radial displacements of the MC3′ by ±5 mm were also not detectable. For solving these issues, a new magnetic configuration to detect the displacement of the two modular coils is proposed in this section. As mentioned in the first section, the CFQS has four electric power supplies to independently apply electric currents to the four differently shaped MCs. The four power supplies can be used as a tool to detect the radial displacement of the coils. The weighted electric current on the two modular coils ((MC1 and MC1′) or (MC3 and MC3′)) can enhance the influence of the error magnetic fields on the magnetic surfaces, making the measurements more sensitive to the radial displacement of the MCs. In the case of the new magnetic configuration for detecting the displacement of MC1′, the electric currents of MC1 and MC1′ are increased to 35.5 kA·T from that in the standard configuration (27.3 kA·T). The electric currents of the other modular coils are decreased to 24.6 kA·T, which is for keeping the total electric currents of all MCs in the new magnetic configuration to that in the standard configuration. In the case of the new magnetic configuration for detecting the displacement of MC3′, the electric currents of MC3 and MC3′ are enhanced with the decreased electric currents of the other MCs.

Figures 9 (a), (b), and (c) present the calculated magnetic surfaces in the new magnetic configuration when the modular coil MC1′ is displaced by −5 mm, 0 mm, and +5 mm in the major radius, respectively. The electric currents of the modular coils MC1 and MC1′ are enhanced. The figures show that the up-down symmetric ($m/n = 6/2$) magnetic islands are formed for no displacement of the coil (Fig. 9 (b)). For the displacements of the MC1′ by −5 mm and +5 mm, the structure of the magnetic islands is up-down asymmetric, as illustrated in Figs. 9 (a) and (c), respectively, demonstrating that the small radial displacements of the MC1′ of ±5 mm can be identified by magnetic surface measurements in the new magnetic configuration.

Figures 10 (a), (b), and (c) indicate the calculated magnetic surfaces in the new magnetic configuration in the case where the MC3′ is radially displaced by −5 mm, 0 mm, and +5 mm, respectively. The electric currents of the MC3 and MC3′ are increased. While up-down symmetric magnetic islands are formed for no displacement of the coil (Fig. 10 (b)), up-down asymmetric magnetic islands are produced for the displacements of the MC3′ by −5 mm and +5 mm as presented in Figs. 10 (a) and (c), respectively. They prove that the small radial displacement

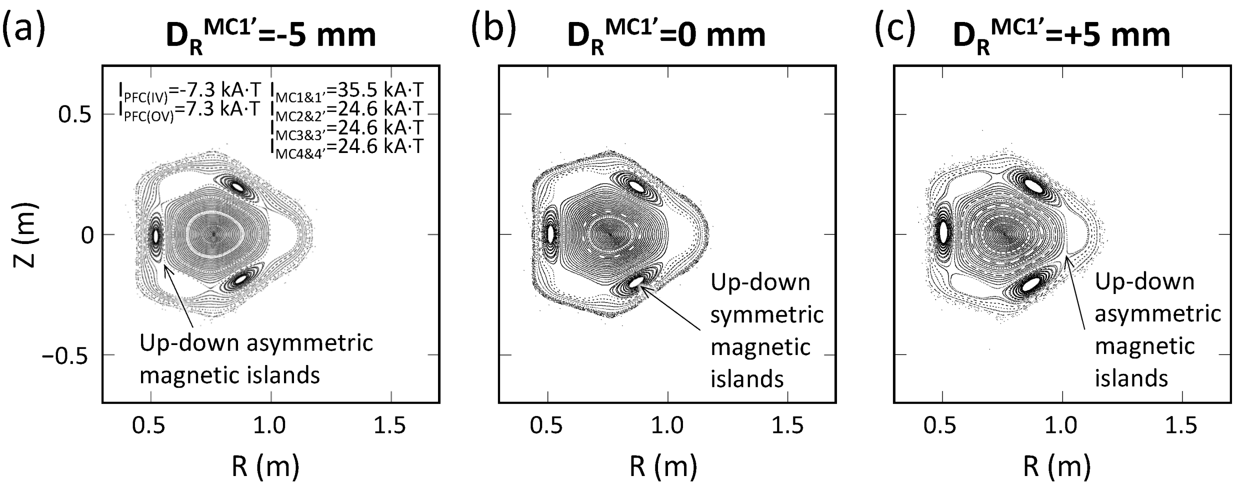

Fig. 9 The calculated magnetic surfaces in the new magnetic configuration to detect the small radial displacements of MC1′ by a weighted electric current on the MC1 and MC1′. The calculations with a radial displacement of the modular coil MC1′ by −5 mm (a), with no displacement (b), and with a radial displacement of the MC1′ by +5 mm are shown.

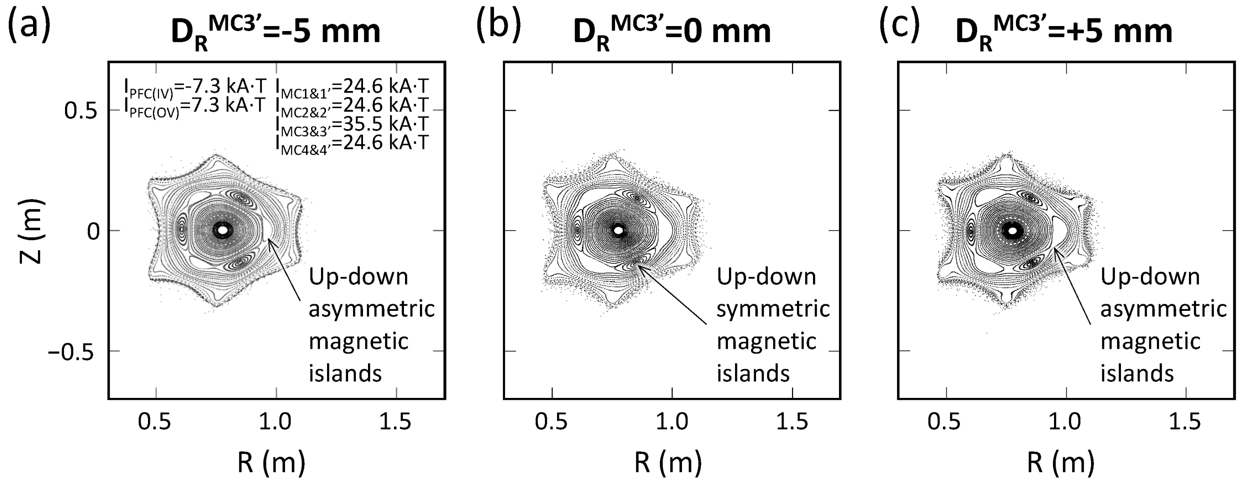

Fig. 10 The calculated magnetic surfaces in the new magnetic configuration to detect the small radial displacements of MC3′ by a weighted electric current on the MC3 and MC3′. The calculations with a radial displacement of the modular coil MC3′ by −5 mm (a), with no displacement (b), and with a radial displacement of the MC3′ by +5 mm are depicted.

of the MC3′ is also detectable in the new magnetic configuration.

6. Summary

It has been found that the magnetic surfaces in the CFQS in the standard magnetic configuration are robust against the error fields, due to the misalignment of the modular coils (MCs). This property is not appropriate for detecting the misalignment of the coils. A magnetic configuration specialized in the magnetic surface measurements using the poloidal field coils (PFCs) was proposed. The calculations by tracing the magnetic field lines demonstrated that the structure of the magnetic islands ($m/n = 6/2$) in the specialized magnetic configuration was sensitive to the error fields caused by a misalignment of the modular coils, such as a radial displacement of the coil by +10 mm in the major radius. The calculations also showed that the small radial displacements of the MC2′ or MC4′ by ±5 mm could be detected by observing the up-down asymmetry of the magnetic islands. However, they indicated that the small radial displacements of the MC1′ or MC3′ were not detectable, even in the specialized magnetic configuration. A new magnetic configuration with a weighted electric current on the modular coils ((MC1 and MC1′) or (MC3 and MC3′)) was proposed, which successfully enabled the detection of the displacement of the MCs by observing the up-down asymmetry of the magnetic islands. It was proved that the small radial displacements of one of all MCs by ±5 mm could be detected by measuring magnetic surfaces in the CFQS.

Acknowledgments

This work was performed by the NIFS-SWJTU joint project (NSJP) under the support of programs of international collaborations with overseas laboratories (UFEX105 and UFEX108). One of the authors (M.S.) appreciates the associated staff of NIFS.

[1] A. Shimizu *et al.*, Nucl. Fusion **62**, 016010 (2022).
[2] S. Okamura *et al.*, Nucl. Fusion **41**, 1865 (2001).
[3] NIFS PROC CFQS Team 2021 NIFS-SWJTU Joint project for CFQS: physics and engineering design ver. 3.1 Research Report NIFS-PROC Series: NIFS-PROC-119 National Institute for Fusion Science.
[4] H. Yamada *et al.*, Rev. Sci. Instrum. **61**, 686 (1990).
[5] O. Motojima *et al.*, Nucl. Fusion **40**, 599 (2000).
[6] A. Iiyoshi *et al.*, Nucl. Fusion **39**, 1245 (1999).
[7] M. Otte *et al.*, Plasma Phys. Control. Fusion **58**, 064003 (2016).
[8] S. Kinoshita *et al.*, Plasma Fusion Res. **14**, 3405097 (2019).
[9] A. Shimizu *et al.*, Plasma Fusion Res. **14**, 3403151 (2019).
[10] A.H. Boozer *et al.*, Plasma Phys. Control. Fusion **50**, 124005 (2008).